Colloids and Surfaces B: Biointerfaces 71 (2009) 138–147

Contents lists available at ScienceDirect

Colloids and Surfaces B: Biointerfaces

journal homepage: www.elsevier.com/locate/colsurfb

AFM measurements of interactions between the platelet integrin receptor GPIIbIIIa and fibrinogen

Aashiish Agnihotri [a], Pranav Soman [a], Christopher A. Siedlecki [a,b,*]

[a] Department of Bioengineering, The Pennsylvania State University, College of Medicine, Biomedical Engineering Institute, Hershey, PA 17033, United States
[b] Department of Surgery, The Pennsylvania State University, College of Medicine, Biomedical Engineering Institute, Hershey, PA 17033, United States

ARTICLE INFO

Article history:
Received 3 November 2008
Received in revised form 24 January 2009
Accepted 25 January 2009
Available online 3 February 2009

Keywords:
Fibrinogen
Platelet membrane integrin
Atomic force microscopy (AFM)
Binding force measurements
Blood–material interactions

ABSTRACT

Binding of receptor proteins on circulating platelets to fibrinogen adsorbed on a biomaterial surface is a critical event in the blood–material interactions and surface-induced thrombogenesis. In this work, the interactions between purified platelet membrane integrin GPIIbIIIa ($\alpha_{IIb}\beta_3$) and fibrinogen on model hydrophilic and hydrophobic surfaces were characterized by measuring ligand–receptor debonding forces by atomic force microscopy (AFM). Force profiles between AFM probes functionalized with platelet integrins and fibrinogen on these substrates showed multiple rupture events over large distances on both surfaces. On the hydrophobic surface, the rupture length range was 20–200 nm, whereas on the hydrophilic surface, the rupture length range was 20–400 nm. Rupture events in the force curves were found to arise from non-specific protein–protein interactions, mechanical denaturation of fibrinogen domains, as well as the specific ligand–receptor interactions between integrins and fibrinogen. Analysis of the distributions of the debonding forces was used to estimate the strength of single integrin–fibrinogen pair at different loading rates. For loading rates of 10–60 nN/s, the debonding strength of a single integrin–fibrinogen pair was found to be in the range of 50–80 pN and was independent of the underlying substrate. Results suggest that once the active platelet binding epitope in fibrinogen becomes exposed by surface adsorption, binding of the platelet membrane integrin receptor will be similar regardless of the material surface properties.

© 2009 Elsevier B.V. All rights reserved.

1. Introduction

The interaction of blood with biomaterial surfaces evokes a number of adverse biological responses including surface-induced thrombosis, a problem that continues to impede the development of hemocompatible biomaterials for long-term blood-contacting applications. Soon after blood contacts the material surface, a layer of plasma proteins forms on the surface that controls subsequent responses [1]. A widely accepted postulate in biomaterials science is that the interactions of proteins with surfaces result in expression of active epitope(s) that can initiate a sequence of biochemical reactions leading to host responses to the biomaterial in contact. In the case of surface-induced thrombosis, adsorption of fibrinogen onto a surface is believed to expose functional epitopes that can interact with the receptors on platelet membranes leading to platelet adhesion, activation, and aggregation [2].

Fibrinogen is the most abundant coagulation protein in blood with a circulating concentration of 2.6–3.5 mg/mL. It has a symmetrical, dimeric structure with two sets of three intertwined polypeptide chains called Aα, Bβ, and γ [3]. The platelet membrane receptor that recognizes fibrinogen is a member of the integrin family, and is composed of a glycoprotein complex of α_{IIb} and β_3 (GPIIbIIIa) [4]. The α_{IIb} (135 kDa) and β_3 (95 kDa) chains form a 1:1 Ca^{2+}-dependent heterodimer in the platelet membrane. GPIIbIIIa can exist in two conformational states and its conformation determines its ligand-binding activity. Resting GPIIbIIIa in an unstimulated platelet does not bind to fibrinogen in solution, and only after GPIIbIIIa is transformed into its activated state is it able to bind soluble fibrinogen [5]. This activation of GPIIbIIIa plays an important role in platelet aggregation in the hemostatic response. Inactive platelet integrins can bind to adsorbed fibrinogen; however, leading to platelet adhesion and activation [6,7].

In general, the binding of a ligand to an integrin is mediated by a short amino acid sequence in the ligand. There are three pairs of linear peptide sequences in fibrinogen through which the protein can potentially bind to GPIIbIIIa. The two RGD pairs in each of the Aα chains (RGDF at 95–98 and RGDS at 572–575) bind predominantly to residues 109–171 in β_3 [8,9], whereas the dodecapeptide sequence at the C-terminal ends of γ chains (HHLGGAKQAGDV,

* Corresponding author at: The Pennsylvania State University, The Milton S. Hershey Medical Center, Biomedical Engineering Institute, Department of Surgery, H151, 500 University Drive, Hershey, PA 17033, United States. Tel.: +1 717 531 5716; fax: +1 717 531 4464.
E-mail address: csiedlecki@psu.edu (C.A. Siedlecki).

0927-7765/$ – see front matter © 2009 Elsevier B.V. All rights reserved.
doi:10.1016/j.colsurfb.2009.01.019

400-411) couples with residues 294–314 in α_{IIb} [10,11]. The dodecapeptide sequences have been shown to be the primary mediators of platelet adhesion to immobilized fibrinogen [12–14] with the last four amino acid residues (AGDV) essential for this function [15].

Protein adsorption to a surface is a complex process governed by several factors, but perhaps most importantly by the material surface properties [16,17]. It has been suggested that surface properties may modulate the subsequent biological response by preferential adsorption of a protein [18–21] and/or influencing the biological activity of the protein [22–24]. The latter could be mediated by either adsorption-induced conformational changes or by alteration of the ligand–receptor-binding kinetics on the surface. We have previously studied the surface- and time-dependent conformational changes in fibrinogen on model hydrophobic and hydrophilic surfaces and found that surface properties clearly impact the conformational changes in fibrinogen on surfaces [25]. Previously, others have studied binding kinetics of fibrinogen–integrin pairs, but in those studies, fibrinogen molecules were covalently attached to a surface [26,27]. It is unclear whether the surface modification for covalent attachment of fibrinogen may influence the surface properties or the conformation of protein. In this study, the influence of surface properties on the interactions between platelet integrin GPIIbIIIa and fibrinogen on surfaces were investigated. The debonding forces between AFM probes modified with purified platelet integrin receptors and fibrinogen on hydrophobic and hydrophilic model surfaces were measured and single integrin–protein interaction forces calculated.

2. Materials and methods

2.1. Materials

Human fibrinogen, >95% pure as stated by the supplier, was obtained as lyophilized powder from Calbiochem (La Jolla, CA). Purified human integrin GPIIbIIIa was purchased from Enzyme Research Labs (South Bend, IN) as an ~2 mg/mL solution in Tris buffer (pH 7.4) stabilized with 50% (v/v) glycerol and 0.1% (v/v) Triton X-100 detergent. Bovine serum albumin (BSA) and the RGD-containing peptide (GRGDSPK) were obtained from Sigma Chemicals Co. (St. Louis, MO). PAC-1, FITC antibody was purchased from Becton Dickinson, San Jose, CA. Coli S69 (IgG_1 isotype control) was obtained from Washington State University Monoclonal Antibody Center (WSUMAC). EDTA was purchased from VWR International (West Chester, PA). Glutaraldehyde was purchased from J.T. Baker (NJ). Aminopropyltriethoxysilane (APTES) was obtained from Gelest Inc. (PA). Muscovite mica, the model hydrophilic surface, was from Ted Pella Inc. (CA), while highly ordered pyrolytic graphite (HOPG, grade II), the model hydrophobic surface, was from Structure Probe Inc. (PA).

All water was from a Millipore Simplicity 185 system with dual UV filters (185 and 254 nm) to reduce carbon contamination. Fibrinogen solution was prepared in 1 mM phosphate buffer (pH 7.4). Integrins were stored in a 20 mM Tris–HCl buffer system with 100 mM NaCl, 1 mM $CaCl_2$, Triton X-100 (0.1%, v/v), and glycerol (50%, v/v). A second Tris buffer supplemented with 2 mM of $MnCl_2$ was also prepared, and probe modification and force measurement experiments were conducted in this buffer. Mn^{2+} induces conformational changes in integrin molecules leading to activation [28,29].

2.2. Probe modification

The long-thin Si_3N_4 triangular cantilevers (Digital Instruments, Santa Barbara, CA) were used for force–distance curve acquisition. Integrins were directly immobilized on the integral tip of the probe after modification with an amine-terminated SAM. Tips were treated in a commercial plasma cleaner (Harrick Sci. Corp., NY) for 15 min (ambient atmosphere, 100 W power) and then incubated in 1% (v/v) solution of APTES in ethanol for 30 min. After thoroughly rinsing with Millipore water, the tips were reacted with glutaraldehyde in 10% aqueous solution for 1 h. The tips were again rinsed with Millipore water and then incubated with either the integrin solution (25 μg/mL in Tris–HCl buffer with Mn^{2+}) overnight at 4 °C or Coli S69A (25 μg/ml), an isotype control for IgG_1 antibodies in PBS buffer at room temperature for 1 h. The modified probes were again thoroughly rinsed and stored in the buffer at 4 °C until use. The aldehyde group of glutaraldehyde forms an imine link with primary amine groups, thereby linking the amine group of the tip surface to primary amine groups on the protein. This linking mechanism has been shown to provide sufficient mobility and flexibility to proteins (receptors/antibodies) to rotate and orient themselves for binding [30–32], and a similar linking mechanism was used by Litvinov et al. [26,33] to immobilize integrin $\alpha_{IIb}\beta_3$ on silica microspheres for optical tweezer studies. The surface density of integrin molecules on the tip was not quantified.

2.3. Atomic force microscopy

AFM data were collected using a Nanoscope IIIa Multimode AFM (Digital Instruments, Santa Barbara, CA). The data were acquired in the adhesion mode (also known as the 'Force-Volume' mode), in which force–distance curves are acquired over a grid of specified size. This allows collection of a large number of force curves in one file that can be analyzed together, and avoids repeated measurements over the same location. Force curves were measured in a 16 × 16 matrix on a 500 nm × 500 nm area, with 512 data points for both the approaching and retracting force curves.

The 'Force-Volume' mode allows measurements of force curves such that the maximum deflection of the cantilever during each force cycle can be kept constant. The maximum deflection of the cantilever determines the contact area between the probe and the surface and the number of bonds formed between integrins on the tip and the adsorbed fibrinogen. The maximum deflection was set to either 50 or 100 nm in these experiments. The ramp size for the force curves (the distance moved by the piezo in one cycle in one direction) was set to 500 nm. The loading rate (spring constant of the cantilever × the retract velocity) was varied between 10 and 60 nN/s by varying the separation velocity of the probe. The nominal value of 0.06 N/m supplied by the manufacturer was used as the spring constant for the probes to convert deflection curves to force curves. Variations in the spring constants of the tips used may add some errors in the calculation of loading rates.

Force curves were first taken against BSA (100 μg/mL) on mica and HOPG substrates in order to characterize the non-specific protein–protein interactions. Fibrinogen (10 μg/mL) was incubated on the HOPG and mica materials for 1 h and the protein solution was replaced with buffer prior to force curve measurements. This replacement step is critical to prevent blocking of the integrins on the probe by any free fibrinogen remaining in the solution. After acquiring force curves at several loading rates, integrins on the tip were blocked by infusing the RGD-containing peptides, and force curves were acquired again. In some experiments, instead of using RGD peptides to block the integrins on the tip, the force curves were acquired in a buffer containing 1 mM EDTA. EDTA is a Ca^{2+} chelator and removes the Ca^{2+} ions from the buffer that are critical for integrin to maintain its active conformation [34]. Therefore, in the presence of EDTA, the integrin loses its ability to bind to ligands.

In other control experiments, force curves were obtained between (a) IgG_1 isotype (Coli S69) modified AFM probe and fibrinogen on the substrates, (b) integrin-modified probes and IgG_1

on mica and (c) integrin-modified probes and PAC-1 antibody (100 μg/mL) on the mica substrates.

2.4. Data analysis

The force curve data were extracted from the AFM files and analyzed off-line with tools developed in MatLab™ (The Mathworks Inc., MA). The retraction (or separation) portion of the force curves obtained with integrin-modified probes against fibrinogen typically had several jumps or rupture events in the non-contact region, potentially corresponding to the debonding of multiple integrin–fibrinogen bonds in several steps. This part of the force curve was analyzed by measuring the local force maxima and minima to obtain the rupture forces corresponding to the individual events. The total debonding force of a particular force curve was the summation of all the local rupture forces at various locations along the force curve. The distances over which the rupture events occur were also evaluated and distributions of these rupture distances were generated. Distributions of the rupture forces at each loading rate were also generated. For plotting of distributions, the debonding forces were categorized into bins of 10 pN size and converted into a probability distribution, where $P(x)$ = (number of debonding events between $x-5$ and $x+5$)/(number of total events).

The periodicity of the peaks in the rupture force distributions was obtained by a program developed in MatLab. In a typical debonding force distribution, several peaks were visible. The number of debonding events in each of the columns was given one of the six values of 'weight' (10, 7, 4, 3, 1, and 0.75), with the absolute peak value of 10. This assignment was based on the height of the column relative to the height of its two nearest neighboring columns on either side.

A range for the expected periodicity (50–99 pN) was selected on the basis of several reports in literature on debonding strength of similar single ligand–receptor interactions [26,35–38]. An estimator was evaluated for each value (ν) that fell within a range of numbers in the vicinity of expected periodicity. Briefly, the estimator was calculated by counting the 'weighted' number of rupture events at the integral multiples of ν and those peaks appearing in the distribution at an integral multiple of ν were given extra weight as described above. The weighting scheme ensures that maximum number of peaks appear at the integral multiples of the periodicity. The rupture events occurring within a ±5 pN range of ν were also added to the estimator in the same fashion to accommodate the error in measurements. The debonding force distributions were plotted with bins of size 10 pN resulting in a maximum error of 20 pN in the estimated periodicities.

The algorithm was tested with two fictitious distributions: one with a perfect periodicity and the second one generated by adding random noise to the first distribution. The same value of periodicity was obtained for both distributions, demonstrating the efficacy of the algorithm.

3. Results and discussion

3.1. Force curve analysis

Force curves were obtained from a series of control experiments in order to evaluate the interactions among (1) bare mica/HOPG substrates and bare probes, (2) bare mica/HOPG substrates and integrin-modified probes, (3) BSA on mica/HOPG and integrin-modified probes and (4) fibrinogen on mica and an AFM probes functionalized with a generic IgG. Force spectroscopy recorded very little-to-no adhesion forces between the bare AFM probes and bare mica/HOPG substrates under PBS buffer (data not shown). Force spectroscopy showed large non-specific adhesion forces between functionalized probes and bare mica/HOPG substrates. Representative force curves showing the interactions between the integrin-modified probes and BSA on mica typically show no rupture events, as illustrated in Fig. 1A. Occasional weak rupture events were also observed in the force curves obtained with integrin-modified probes on BSA, and these are attributed to proteins adhering through non-specific interactions. In contrast, the interactions of integrin-modified probes with fibrinogen on mica show large rupture events (Fig. 1B). Fig. 2 summarizes the force distribution profiles for the interactions between functionalized AFM probes and BSA on HOPG (Fig. 2A) and mica (Fig. 2B). Most of these non-specific rupture forces were found to be in the range of 0–150 for both substrates, lower in magnitude than the forces typically observed for fibrinogen on these same substrates (Fig. 2C and D), where most rupture forces lie in the range of 10–550 pN on HOPG (Fig. 2C) and 0–350 pN on mica (Fig. 2D). We find a substantial increase in the debonding forces when compared to the non-specific BSA distributions (typically 0–150 pN). This result shows that there are enough differences between BSA–integrin non-specific interactions and fibrinogen–integrin specific interactions. Force distributions between AFM probes functionalized with a generic control IgG and fibrinogen on mica substrates were found in the range of 0–70 pN, substantially lower than the non-specific BSA controls (data not shown).

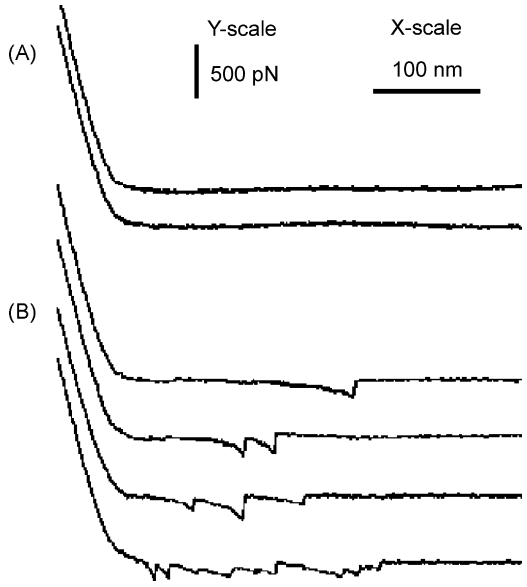

Fig. 1. Typical force curves with integrin-modified probes against BSA on mica (A) showing no specific or non-specific adhesive interactions and fibrinogen on mica (B) showing rupture events potentially due to the debonding of integrin–fibrinogen pairs.

The percentages of force curves showing rupture events under different experimental conditions are summarized in Fig. 3. For BSA on mica, rupture events were detected in 13.7 ± 6.8% (mean ± standard deviation) of the force curves. When force curves were acquired with the integrin-modified probe against fibrinogen on mica, the number of force curves showing rupture events rose to 48.5 ± 11.5%. Similarly, when force curves were acquired on fibrinogen on HOPG, rupture events were observed in 58.2 ± 8.2% force curves. An increase in the number of force curves showing rupture events for fibrinogen on mica and HOPG as compared to the number of rupture events against BSA controls suggests an increased interaction of the integrins on the tip with the fibrinogen molecules, attributable to ligand–receptor interactions between the integrins and fibrinogen. To verify this further, force curves were acquired after blocking the integrins on the tip with an RGD-

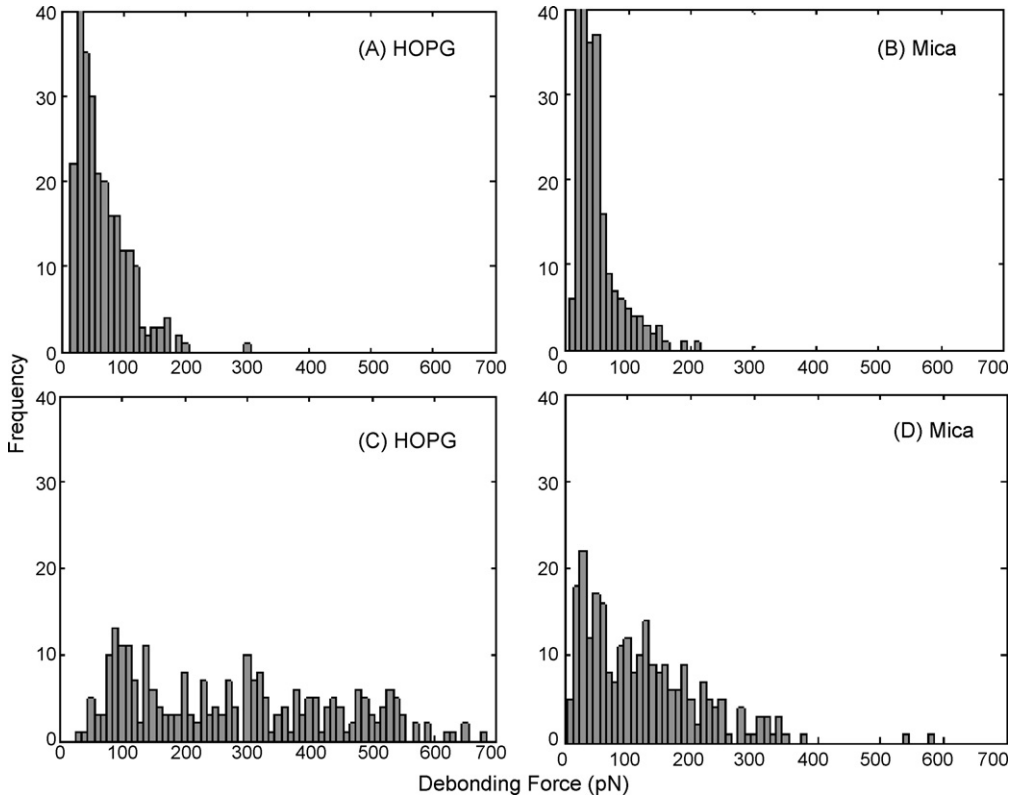

Fig. 2. Typical force distributions with integrin-modified AFM probes against BSA on HOPG (A) and mica (B) substrates, both showing debonding forces in the range of 0–150 pN; and for fibrinogen on HOPG (C) and mica (D) showing debonding forces in the range of 20–700 pN and 0–370 pN, respectively.

containing peptide or in the presence of EDTA in the buffer. The number of force curves showing rupture events after blocking of interactions on mica dropped to 40.5 ± 19.8%. Due to the large standard deviation, no statistically significant decrease in the percent of force curves showing rupture events after blocking could be established. However, this could be due to inefficient blocking of the specific interactions as well as to contributions from non-specific interactions, suggesting that in the case of force curves between an integrin-modified probe and adsorbed fibrinogen, the rupture events were due to both the specific and non-specific interactions of proteins.

For the force curves that showed rupture events, the number of rupture events per force curve also varied (Fig. 4). On HOPG, the average number of rupture events per force curve was 3.3 ± 1.9 (mean ± standard deviation), whereas on mica, the average number of rupture events per force curve was 1.7 ± 1.1. Again, the number of rupture events observed per force curve for the integrin-modified probes against fibrinogen on HOPG and mica, and after blocking, was not statistically distinguishable, although the trends indicate a decrease, albeit with large variability.

3.2. Rupture length analysis

As shown in Fig. 1B, the rupture events were observed over a large range of distances from the surface. To compare the rupture distances for different materials, rupture lengths were calculated from the surface of the substrate as illustrated in Fig. 5. The position of the substrate in the force curve was estimated from the approach portion of the force curve. As the cantilever approaches the surface, it begins deflecting when it comes into contact with either proteins or the surface itself. The position of the surface of the substrate was calculated as the intersection point of straight lines fit to the

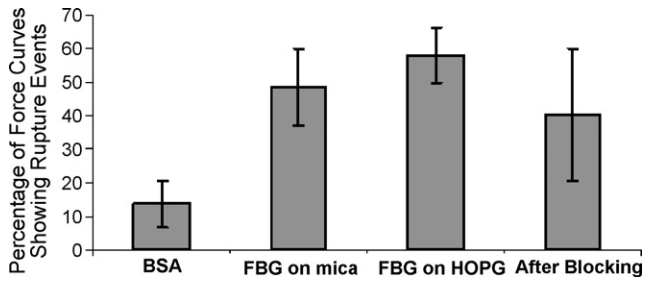

Fig. 3. Percentage of force curves showing rupture events as acquired with integrin-modified probes against BSA on mica, fibrinogen on mica and HOPG, and fibrinogen on mica following blocking the integrins with an RGDS-containing peptide. (Error bars are standard deviations.)

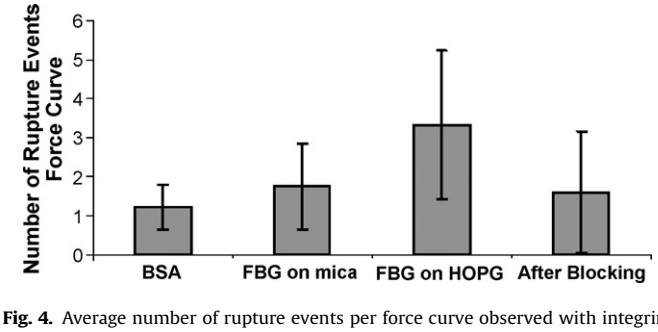

Fig. 4. Average number of rupture events per force curve observed with integrin-modified probes against BSA on mica, fibrinogen on mica and HOPG, and fibrinogen on mica following blocking the integrins with an RGDS-containing peptide. Only the force curves showing a rupture event were used in the calculation. (Error bars are standard deviations.)

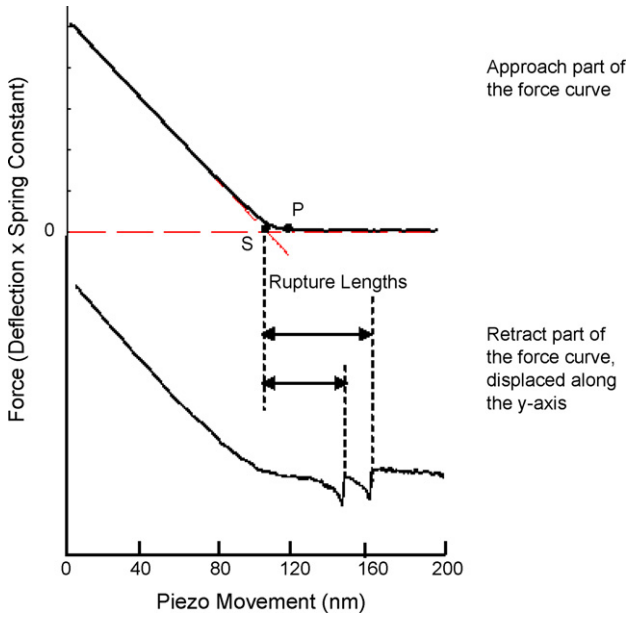

Fig. 5. Illustration of rupture length calculation. The z-position of the substrate surface is estimated from the approach portion of the force curve. The cantilever starts deflecting at point P, the surface of the protein layer, and this deflection is accompanied by tip indentation into the protein layer. The piezo position of the substrate surface is estimated by extrapolating the non-contact and the linear contact regions of the approaching force curve. The retracting portion of the force curve is shown displaced along the *y*-axis for clarity. The rupture lengths are calculated by subtracting the piezo position of the substrate surface from the position of the rupture event.

non-contact portion of the force curve and the linear portion of the contact region of the force curve. In Fig. 5, the retracting portion of the force curve showing the rupture events has been displaced along the *y*-axis for clarity.

Distributions of rupture lengths were plotted for each loading rate for both surfaces. On HOPG, the rupture events were generally observed in 20–200 nm range (Fig. 6). The range of the rupture length on mica was 20–400 nm, almost double of that on HOPG, with a substantial number of those rupture events occurring at distances greater than 200 nm (Fig. 7).

The length of a fibrinogen molecule is ~48 nm and the integrin molecule with its head and tail combined stands ~34 nm long. The observed values of rupture length are much higher than these two molecules combined, suggesting stretching or extension of either fibrinogen, integrin, or both, on the tip. Similar stretching has been seen in other studies using antibodies against fibrinogen [30,32].

The integrin molecules on the tip remained functional even after measurement of over 1000 force curves, suggesting that its structure, which is critical for its ligand-binding activity, was more or less preserved. This also demonstrates that fibrinogen does not remain bound to the integrin and is not pulled away from the surface. If the fibrinogen molecules are undergoing stretching, then this must be accompanied by mechanical denaturation of one or more of the individual domains in the protein. When fibrinogen binds to integrins on the AFM probe, regions of the molecule might temporarily leave the surface and then return after ligand–receptor rupture. This kind of mechanical unfolding of single proteins has been studied by AFM, most notably for the giant muscle protein titin [39,40], where the rupture events due to unfolding of individual domains were observed at periodic distances. Such unfolding curves can be analyzed by using analytical models of force-induced unfolding of proteins such as the worm-like-chain (WLM) model of polymer elasticity [41]. In this case, in addition to unfolding of protein domains, the rupture signal may be due to debonding of integrin–fibrinogen bonds and non-specific protein–protein interactions, therefore a simple analytical model can not be used to analyze the force curves.

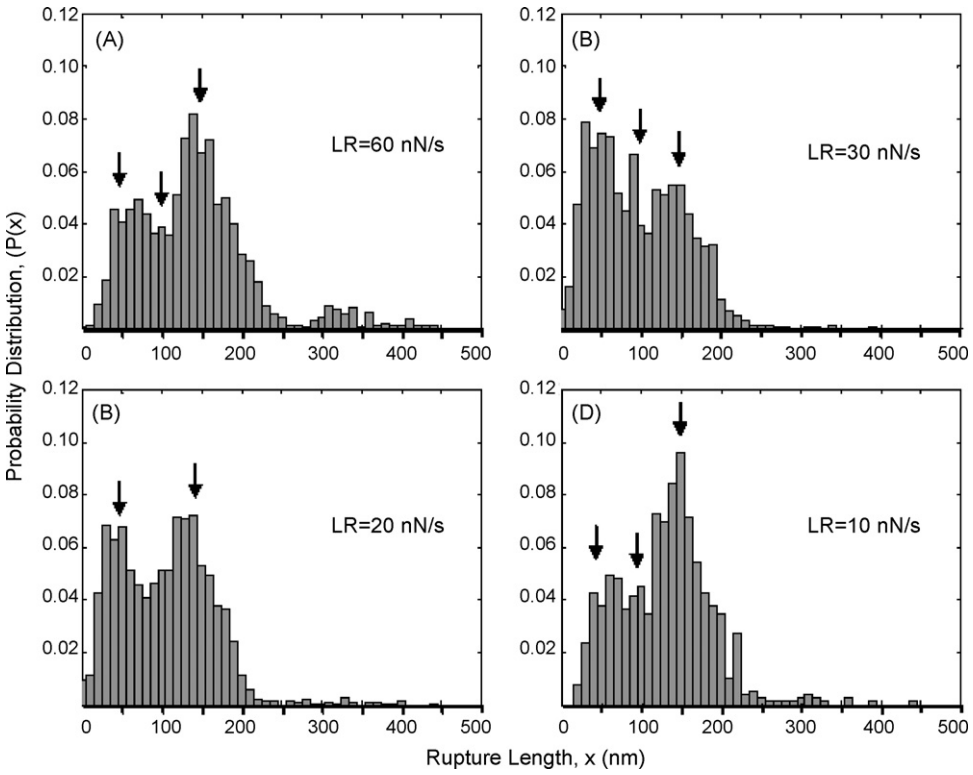

Fig. 6. Distributions of rupture length for force curves taken with integrin-modified probes against fibrinogen on HOPG at different loading rates (LR): (A) LR = 60 nN/s, (B) LR = 30 nN/s, (C) LR = 20 nN/s, and (D) LR = 10 nN/s. A majority of rupture lengths occurred in the range of 20–200 nm from the HOPG surface. The rupture events could be partitioned into three clusters, around rupture lengths of 50, 100, and 150 nm.

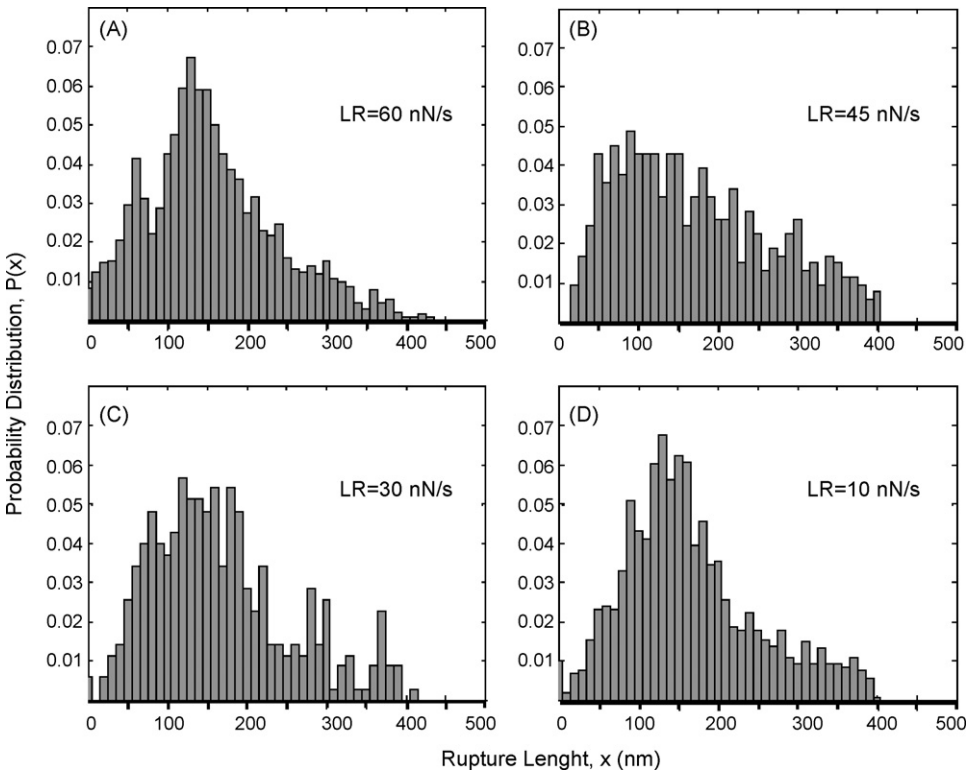

Fig. 7. Distributions of rupture length for force curves taken with integrin-modified probes against fibrinogen on mica at different loading rates (LR): (A) LR = 60 nN/s, (B) LR = 45 nN/s, (C) LR = 30 nN/s, and (D) LR = 10 nN/s. The range of rupture lengths has increased to 20–400 nm compared to the HOPG substrate.

While studying the adsorption of fibrinogen on model surfaces with varying chemistry, Sethuraman et al. [42] also observed similar rupture events in the force curves, which they attributed to mechanical denaturation of fibrinogen. In that study, the extension and observed rupture events were due to adhesion to the surface and not due to specific interaction with its receptor.

The difference in the range of rupture length on mica and HOPG is an interesting observation. It indicates that at least a part of the fibrinogen population undergoes mechanical denaturation through a different pathway or to a greater extent on the hydrophilic surface as compared to the hydrophobic material. The origin of this difference is not clearly understood. Two possibilities are discussed below.

In thermal denaturation studies, it has been shown that the E domain and coiled coil regions are relatively thermostable, whereas the D and αC domains (which is an independent domain near the central E domain) are thermolabile, suggesting that the D and αC domains have lower structural stability [43]. This suggests that as the integrin on the probe that has formed a bond with an adsorbed fibrinogen through its γ chain dodecapeptide (in the D domain) starts pulling the fibrinogen, the D domain should be the first to unfold. The D domain is composed of two distinct globular nodules corresponding to the C-terminus of the γ and Bβ chains. As fibrinogen adsorbs to the hydrophobic HOPG surface quite strongly [25,44], it is possible that only one of the nodules in the D domain can undergo stretching on this surface. However, on the hydrophilic mica surface, fibrinogen is only weakly adherent and the weaker protein–surface interaction may allow both nodules of the D domain to unfold.

An alternate explanation demands to consider the adsorbed protein layer as a three-dimensional construct instead of a two-dimensional plane and include the solvent, water, in the analysis. It has been shown that a water layer may exist between proteins and a hydrophilic mica surface [30,45,46]. On the basis of the larger range of rupture distances on mica, it could be postulated that the interfacial region, where the fibrinogen molecules are associated with the surface, is thicker on the hydrophilic mica surface than on the hydrophobic HOPG surface. At this time, the data do not suggest one of these alternatives over the other.

3.3. Debonding force analysis

To determine the strength of a single ligand–receptor bond, statistical distributions of the force corresponding to the rupture events were plotted for each loading rate. The debonding forces between an integrin-modified probe and fibrinogen adsorbed onto HOPG and mica were converted into a probability distribution as illustrated in Fig. 8.

If the rupture events represent breaking of integrin–fibrinogen bonds (one, two, or more), then the peaks in the rupture force distributions will occur at integral multiples of the bond strength of a single integrin–fibrinogen pair. The first peak would correspond to the breaking of one pair; the second peak would correspond to two bonds, and so on. On a randomly oriented adsorbed fibrinogen structure, there can be one or more rupture events depending upon the orientation of adsorbed fibrinogen. However, since we calculate the total force, which is the summation of individual forces in a single force curve, the peaks in the force distributions should correspond to the number of rupture events.

The length of the linker molecule is ~50 nm, so there is a possibility of having more than one integrin molecule interacting with the adsorbed fibrinogen. With an increase in the number of interactions or rupture events, there will be corresponding increase in the total rupture force. This method of analysis will still work because the total force will still be a multiple of a single fibrinogen–integrin bond.

However, due to the noise level in our measurements (~50 pN as measured from the base line fluctuations), the first peak (and sometimes the second peak as well) in the rupture force distributions could not be resolved from the noise. The debonding events

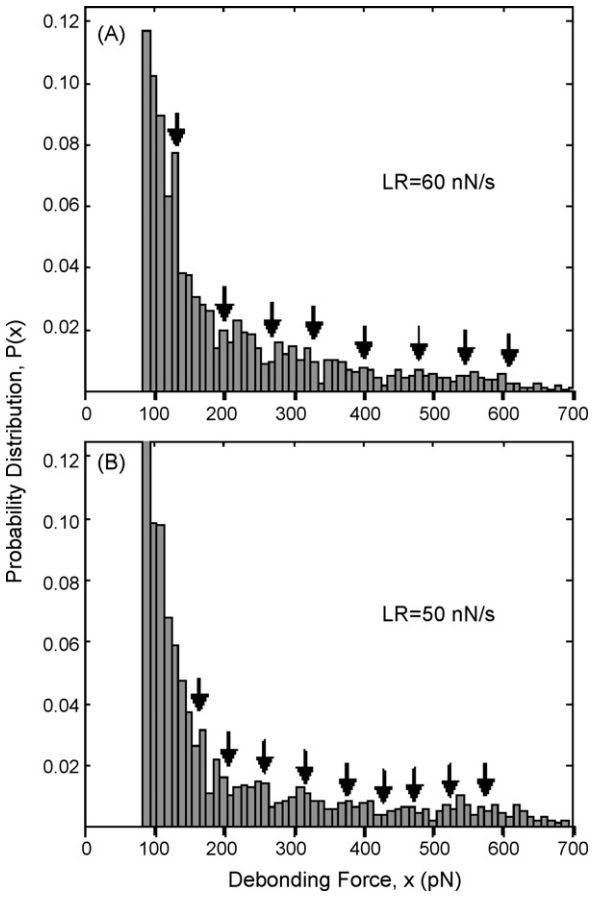

Fig. 8. Probability distribution of debonding force between integrins immobilized on the AFM tips and fibrinogen on a hydrophobic HOPG surface at loading rates (LR) of (A) 60 nN/s and (B) 50 nN/s. Debonding events have been partitioned into bins of 10 pN size and converted to probability distribution as $P(x)$ = (number of events in the bin at x)/(total number of events). The total numbers of rupture events are 1767 for (A) and 1725 for (B) in 768 force curves. The arrow indicates the location of integral multiples of the estimated periodicity (68 pN at LR = 60 nN/s and 53 pN at LR = 50 nN/s). Note that measurements <85 pN are not included due to potential noise artifacts at this level.

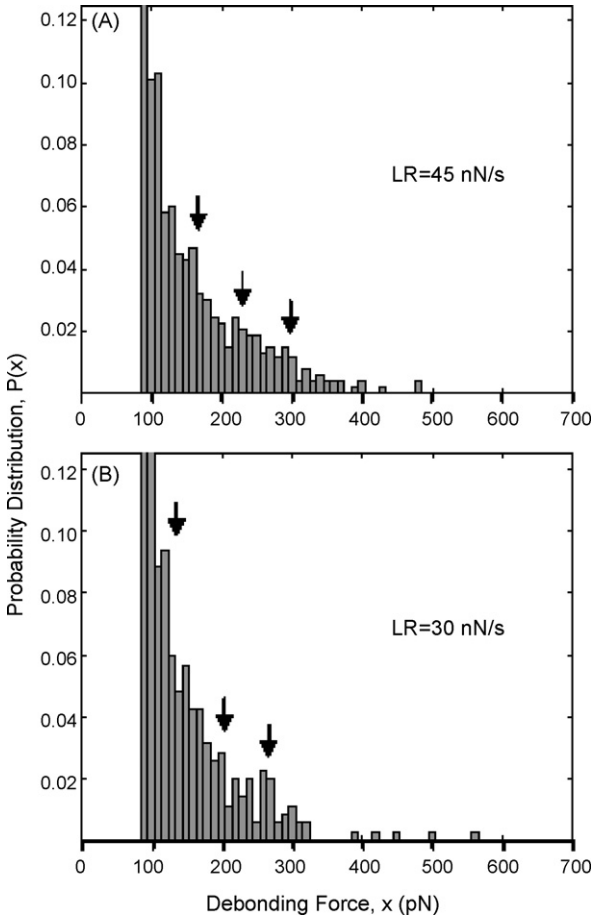

Fig. 9. Probability distribution of debonding force between integrins immobilized on AFM tips and fibrinogen on a mica surface at loading rates (LR) of (A) 45 nN/s and (B) 30 nN/s. The total numbers of rupture events are 533 for (A) and 352 for (B) in 512 force curves. The arrow indicates the location of integral multiples of the estimated periodicity (77 pN at LR = 45 nN/s and 63 pN at LR = 30 nN/s). Force measurements <85 pN are not included due to potential noise artifacts at this level.

below 85 pN were not included in these distributions, as a sharp increase was observed in the number of debonding events below 85 pN, which did not result in any peak and presumably arise largely from noise in the system. Therefore, only the events with rupture force >85 pN were included in analysis, and the periodicity of the peaks observed in the distribution was obtained as the measure of the bond strength of a single integrin–fibrinogen pair (Fig. 9). Moreover, from Fig. 2, it is clear that the exclusion of events below 85 pN will also eliminate many of the non-specific interactions.

In these distributions of debonding forces, several peaks were observed but no distinct periodicity was visible directly. If all the rupture events corresponded to debonding of one or more integrin–fibrinogen pairs, then it would be expected that peaks would occur only at the integral multiples of the debonding force for a single integrin–fibrinogen pair. However, as discussed earlier, some of the rupture events may be due to the non-specific interactions of the proteins, and the long rupture lengths that were observed suggest that some events correspond to stretching and/or mechanical denaturation of one or more domains of fibrinogen. Denaturation or unfolding of a single domain in a protein is typically a one-step process with an activation energy barrier and results in a jump or a rupture event in the force curve that will be similar to debonding of specific fibrinogen–integrin bonds. Therefore, it seems likely that the debonding force distribution contains contributions from debonding of integrin–fibrinogen pairs, rupture of proteins interacting with non-specific interactions, and mechanical denaturation of fibrinogen domains. This may explain a lack of clear periodicity in the debonding force distributions.

Non-specific interactions should not yield a periodic rupture force distribution. By making the assumption that the mechanical denaturation will also not result in a periodic distribution of rupture force, it can be concluded that the rupture force distributions for integrin-modified probes and adsorbed fibrinogen contains a periodic distribution due to debonding of integrin–fibrinogen pairs and some non-periodic 'noise' arising from the non-specific interactions and the mechanical denaturation of fibrinogen.

The algorithm estimates a best-fit periodicity for the rupture force distribution in an expected range, 50–99 pN, selected based on literature. The periodicities that are attributed to the debonding force of a single fibrinogen–integrin pair were extracted using an algorithm that maximizes the number of peaks counted towards the estimation of the periodicity. The periodicity values for the different loading rates are presented in Table 1. With the error associated in the periodicities as well as the loading rates, we could not ascertain the trend of a linear increase in the debonding strength with the logarithm of loading rate as predicted by the Bell model [47]. However, comparison of the debonding strength at the same loading rates on mica and HOPG suggests that there is no difference in the debonding strength for integrins and fibrinogen adsorbed to these two surfaces. From this analysis, it can be concluded that the

Table 1
Debonding strength of a single integrin–fibrinogen pairs at different loading rates.

Loading rate (nN/s)	Debonding strength with integrin-modified probe	
	Fibrinogen adsorbed onto mica (pN)	Fibrinogen adsorbed onto HOPG (pN)
10	57	63
30	63	52
60	70	68

Maximum error in the estimated debonding strengths = 20 pN.

debonding strength of a single integrin–fibrinogen pair lies in the range of 50–80 pN for loading rates 10–60 nN/s on both surfaces.

Litvinov et al. [26] used optical tweezers to study the biomolecular interactions between fibrinogen and integrin. They reported that rupture forces for individual fibrinogen molecules with integrins were 60–150 pN with peak yield strength of 80–100 pN. The loading rate used in this study was ~20 nN/s. In that study, the measurements were not performed in aqueous conditions. Lee and Marchant [37,38] used AFM to measure the force required to rupture bonds between an immobilized RGD and dodecapeptide containing peptides and integrins on the surface of an adherent platelets. They reported a value of ~93 pN as the fundamental debonding force of an individual molecular interaction between the RGD-peptide-modified tip and integrin at a loading rate of 12 nN/s.

The debonding strengths measured here are consistent with these previous studies, although a direct comparison of the results from this study with other studies should be considered carefully because of substantial differences in the experimental protocols. For example, in this work, fibrinogen was physisorbed to the model hydrophobic and hydrophilic surfaces and not chemically coupled. However, for these two surfaces, no difference could be found in the debonding strengths, suggesting that once the adsorbed fibrinogen exposes the critical platelet binding epitope(s) on a surface, binding to the integrin receptors on platelets will have the same interaction strength and follow the same kinetics regardless of the surface properties. In other words, even though total debonding force differs for both surfaces, the strength of each integrin–fibrinogen bond remains the same. Therefore, surface properties will influence platelet adhesion only by modulating the expression of the receptor-binding epitopes in fibrinogen. In the light of the above result, this would mean that an increased number of functional platelet binding epitopes are available for integrin binding on hydrophobic surfaces as compared to hydrophilic surfaces.

It should be noted that the debonding strengths measured in this study were between fibrinogen and 'activated' integrins. Control experiments were conducted to verify that the integrins on the AFM probe were indeed in their activated state, and these results are summarized in Fig. 10. Fig. 10A shows characteristic high debonding forces between bare mica and modified probe. Debonding forces between control protein, BSA and modified probes lie in the range of 0–200 pN (Fig. 10B). PAC-1 recognizes an epitope on the GPIIbIIIa complex of activated platelets at or near the platelet fibrinogen receptor and binds only to activated platelets and is specific for this recognition site within GPIIbIIIa [48]. Debonding forces between PAC-1 physisorbed on mica and modified AFM probe were in the range of 350–850 pN, which unequivocally showed that the integrin receptors on the AFM probe were in their "activated" state. A generic IgG, Coli S69 which does not recognize any platelet receptor was used as another non-specific negative control. Force distributions were substantially lower (0–350 pN) than specific PAC-1 and integrin interactions (Fig. 10D), which suggested an "activated" state of platelet receptors attached to the AFM probe. It may be possible that the integrins in inactive form on unstimulated platelets will interact with adsorbed fibrinogen through different epitopes and with different debonding strengths, but that data are not easily

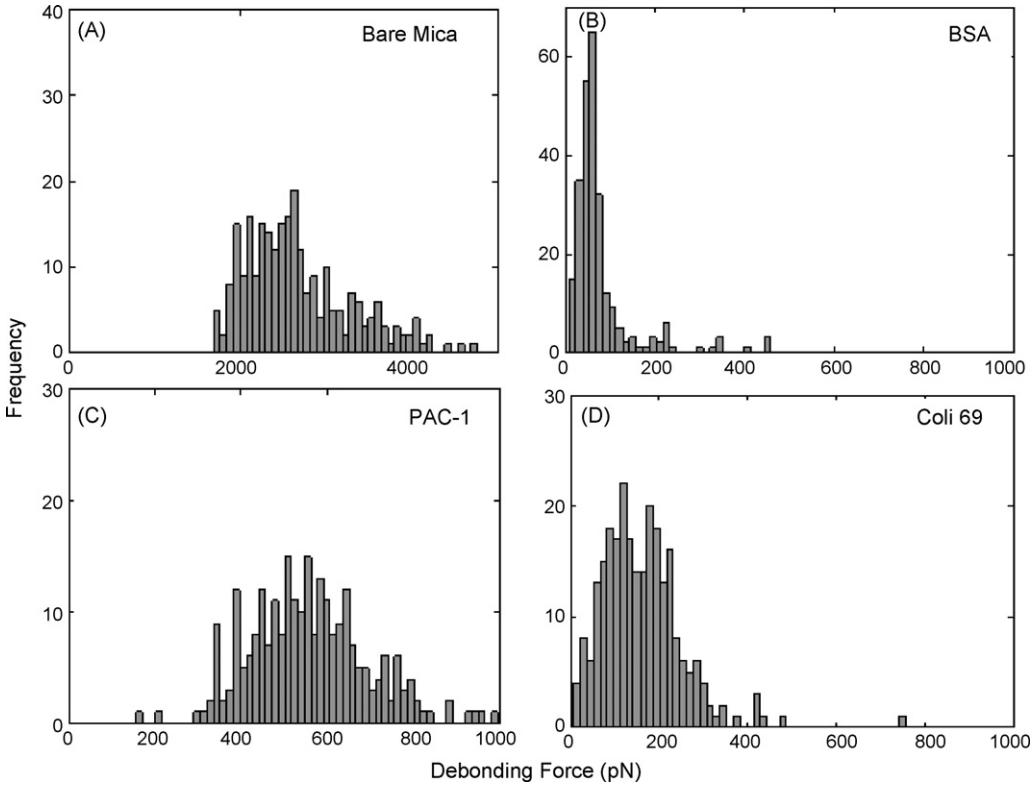

Fig. 10. Debonding force distributions between integrin-modified AFM probe against mica substrate (A), BSA on mica (B), PAC-1 on mica (C) and IgG1 isotype control on mica (D). Force distribution on bare mica (1800–4500 pN) is characteristic of non-specific adhesive debonding forces. Force distributions with control proteins, BSA (0–200 pN) and IgG (0–350 pN) are below the debonding force distribution between PAC-1 antibody and integrin-modified probe (350–850 pN) confirming that the integrins on the AFM probe are in their "activated" state.

available due to significant difficulties in keeping purified integrins in an inactive conformation.

The results illustrated in this paper suggest that the binding strength of platelet integrins to fibrinogen ligands is independent of the wettability of the substrate. If this is the case, then the controlling factor in platelet adhesion to materials is the number of available platelet binding epitopes. A recent paper [32] showed that the exposure of the platelet binding epitope as measured by AFM correlated well with macroscale platelet binding. If the binding strength is not affected by surface properties, then the only way a material can influence platelet adhesion is by changing the probability of the platelet binding epitope being exposed and available. There are two ways in which this probability could be altered. First, there could be an increase in the total amount of fibrinogen adsorbed to the surface, thereby simply increasing the number of fibrinogen molecules that might be in an active conformation and suitable for serving as a platelet ligand. Second, the material could alter the probability that a fibrinogen molecule takes on an active conformation, thereby either increasing or decreasing the number of platelet binding epitopes available for a fixed amount of adsorbed fibrinogen. At this point, we have insufficient data to determine whether one of these mechanisms is the dominant factor in determining blood–material compatibility.

4. Conclusions

The specific interactions between purified and activated integrins with fibrinogen adsorbed onto model hydrophobic and hydrophilic surfaces were studied in aqueous environments by force mode AFM. The range of rupture length on the hydrophobic HOPG surface was 20–200 nm, while the range on the hydrophilic mica surface was substantially larger at 20–400 nm. The rupture events observed in these force curves appear to be attributable to three types of events: non-specific protein–protein interactions, mechanical denaturation of fibrinogen domains, and specific ligand–receptor interactions between the integrins on the probe and adsorbed fibrinogen. The debonding strength of a single integrin–fibrinogen pair was extracted from the periodicity of the debonding force distributions for loading rates in the range of 10–100 nN/s. Debonding strengths were observed in the range of 50–80 pN for these loading rates on both hydrophobic and hydrophilic surfaces, consistent with previous reports. An important physiological implication of these results is that the surface properties appear to therefore influence platelet adhesion only by modulating the expression of critical epitopes in the adsorbed fibrinogen. Once the receptor-binding epitope is available, then binding of the platelet membrane receptor will follow the same kinetics regardless of the surface properties.

Acknowledgements

The authors would like to acknowledge financial support from the National Science Foundation (DMR-0804873), the Biomedical Engineering Institute at the Pennsylvania State University College of Medicine, and the Materials Research Institute at the Pennsylvania State University. We would also like to thank Dr. Lichong Xu for valuable technical discussions.

References

[1] J.L. Brash, T.A. Horbett, Proteins at Interfaces. II. Fundamentals and Applications, American Chemical Society, Washington DC, 1994.
[2] T.A. Horbett, Principles underlying the role of adsorbed plasma-proteins in blood interactions with foreign materials, Cardiovasc. Pathol. 2 (1993) S137–S148.
[3] R.R. Hantgan, P.J. Simpson-Haidaris, C.W. Francis, V.J. Marder, Fibrinogen structure and physiology, in: R.W. Colman, J. Hirsh, V.J. Marder, A.W. Clowes, J.N. George (Eds.), Hemostasis and Thrombosis: Basic Principles and Clinical Practice, Lippincott Williams and Wilkins, Philadelphia, 2001, pp. 203–232.
[4] E.F. Plow, S.J. Shattil, Integrin GPIIb/IIIa and platelet aggregation, in: R.W. Colman, J. Hirsh, V.J. Marder, A.W. Clowes, J.N. George (Eds.), Hemostasis and Thrombosis: Basic Principles and Clinical Practice, Lippincott Williams and Wilkins, Philadelphia, 2001, pp. 479–491.
[5] S.J. Shattil, Signaling through platelet integrin alpha IIb beta 3: inside-out, outside-in, and sideways, Thromb. Haemost. 82 (1999) 318–325.
[6] N. Kieffer, L.A. Fitzgerald, D. Wolf, D.A. Cheresh, D.R. Phillips, Adhesive properties of the beta 3 integrins: comparison of GP IIb-IIIa and the vitronectin receptor individually expressed in human melanoma cells, J. Cell Biol. 113 (1991) 451–461.
[7] B. Savage, Z.M. Ruggeri, Selective recognition of adhesive sites in surface-bound fibrinogen by glycoprotein IIb-IIIa on nonactivated platelets, J. Biol. Chem. 266 (1991) 11227–11233.
[8] S.E. D'Souza, M.H. Ginsberg, T.A. Burke, S.C. Lam, E.F. Plow, Localization of an Arg-Gly-Asp recognition site within an integrin adhesion receptor, Science 242 (1988) 91–93.
[9] S.A. Santoro, W.J. Lawing Jr., Competition for related but nonidentical binding sites on the glycoprotein IIb-IIIa complex by peptides derived from platelet adhesive proteins, Cell 48 (1987) 867–873.
[10] S.E. D'Souza, M.H. Ginsberg, T.A. Burke, E.F. Plow, The ligand binding site of the platelet integrin receptor GPIIb-IIIa is proximal to the second calcium binding domain of its alpha subunit, J. Biol. Chem. 265 (1990) 3440–3446.
[11] S.E. D'Souza, M.H. Ginsberg, G.R. Matsueda, E.F. Plow, A discrete sequence in a platelet integrin is involved in ligand recognition, Nature 350 (1991) 66–68.
[12] D.H. Farrell, P. Thiagarajan, Binding of recombinant fibrinogen mutants to platelets, J. Biol. Chem. 269 (1994) 226–231.
[13] E.F. Plow, T.K. Haas, L. Zhang, J. Loftus, J.W. Smith, Ligand binding to integrins, J. Biol. Chem. 275 (2000) 21785–21788.
[14] W.B. Tsai, J.M. Grunkemeier, T.A. Horbett, Variations in the ability of adsorbed fibrinogen to mediate platelet adhesion to polystyrene-based materials: a multivariate statistical analysis of antibody binding to the platelet binding sites of fibrinogen, J. Biomed. Mater. Res. 67A (2003) 1255–1268.
[15] M.M. Rooney, L.V. Parise, S.T. Lord, Dissecting clot retraction and platelet aggregation. Clot retraction does not require an intact fibrinogen gamma chain C terminus, J. Biol. Chem. 271 (1996) 8553–8555.
[16] W. Norde, J. Lyklema, Why proteins prefer interfaces, J. Biomater. Sci. Polym. Ed. 2 (1991) 183–202.
[17] M. Malmsten, Formation of adsorbed protein layers, J. Colloid Interf. Sci. 207 (1998) 186–199.
[18] T.A. Horbett, P.K. Weathersby, Adsorption of proteins from plasma to a series of hydrophilic–hydrophobic copolymers. I. Analysis with the in situ radioiodination technique, J. Biomed. Mater. Res. 15 (1981) 403–423.
[19] N.P. Ziats, D.A. Pankowsky, B.P. Tierney, O.D. Ratnoff, J.M. Anderson, Adsorption of Hageman factor (factor XII) and other human plasma proteins to biomedical polymers, J. Lab. Clin. Med. 116 (1990) 687–696.
[20] L. Stanislawski, B. De Nechaud, P. Christel, Plasma protein adsorption to artificial ligament fibers, J. Biomed. Mater. Res. 29 (1995) 315–323.
[21] T.A. Horbett, Mass action effects on competitive adsorption of fibrinogen from hemoglobin solutions and from plasma, Thromb. Haemost. 51 (1984) 174–181.
[22] V. Balasubramanian, N.K. Grusin, R.W. Bucher, V.T. Turitto, S.M. Slack, Residence-time dependent changes in fibrinogen adsorbed to polymeric biomaterials, J. Biomed. Mater. Res. 44 (1999) 253–260.
[23] A. Sethuraman, G. Belfort, Protein structural perturbation and aggregation on homogeneous surfaces, Biophys. J. 88 (2005) 1322–1333.
[24] L. Baugh, V. Vogel, Structural changes of fibronectin adsorbed to model surfaces probed by fluorescence resonance energy transfer, J. Biomed. Mater. Res. A 69 (2004) 525–534.
[25] A. Agnihotri, C.A. Siedlecki, Time-dependent conformational changes in fibrinogen measured by atomic force microscopy, Langmuir 20 (2004) 8846–8852.
[26] R.I. Litvinov, H. Shuman, J.S. Bennett, J.W. Weisel, Binding strength and activation state of single fibrinogen–integrin pairs on living cells, Proc. Natl. Acad. Sci. U.S.A. 99 (2002) 7426–7431.
[27] H.L. Goldsmith, F.A. McIntosh, J. Shahin, M.M. Frojmovic, Time and force dependence of the rupture of glycoprotein IIb-IIIa-fibrinogen bonds between latex spheres, Biophys. J. 78 (2000) 1195–1206.
[28] M. Shimaoka, J. Takagi, T.A. Springer, Conformational regulation of integrin structure and function, Annu. Rev. Biophys. Biomol. Struct. 31 (2002) 485–516.
[29] J. Takagi, B.M. Petre, T. Walz, T.A. Springer, Global conformational rearrangements in integrin extracellular domains in outside-in and inside-out signaling, Cell 110 (2002) 511–599.
[30] A. Agnihotri, C.A. Siedlecki, Adhesion mode atomic force microscopy study of dual component protein films, Ultramicroscopy 102 (2005) 257–268.
[31] P.B. Chowdhury, P.F. Luckham, Probing recognition process between an antibody and an antigen using atomic force microscopy, Colloid Surf. A: Physicochem. Eng. Aspects 143 (1998) 53–57.
[32] P. Soman, Z. Rice, C.A. Siedlecki, Measuring the time-dependent functional activity of adsorbed fibrinogen by atomic force microscopy, Langmuir 24 (2008) 8801–8806.
[33] R. Litvinov, G. Vilaire, J. Bennett, H. Shuman, J. Weisel, Ligand-binding activity of individual integrin receptors quantified using optical tweezers-based force spectroscopy, FASEB J. 18 (2004) C69–C169.
[34] L.F. Brass, S.J. Shattil, T.J. Kunicki, J.S. Bennett, Effect of calcium on the stability of the platelet membrane glycoprotein IIb-IIIa complex, J. Biol. Chem. 260 (1985) 7875–7881.

[35] P.P. Lehenkari, M.A. Horton, Single integrin molecule adhesion forces in intact cells measured by atomic force microscopy, Biochem. Biophys. Res. Commun. 259 (1999) 645–650.
[36] E. Kokkoli, S.E. Ochsenhirt, M. Tirrell, Collective and single-molecule interactions of alpha(5)beta(1) integrins, Langmuir 20 (2004) 2397–2404.
[37] I. Lee, R.E. Marchant, Molecular interaction studies of hemostasis: fibrinogen ligand–human platelet receptor interactions, Ultramicroscopy 97 (2003) 341–352.
[38] I. Lee, R.E. Marchant, Force measurements on the molecular interactions between ligand (RGD) and human platelet alpha(IIb) beta(3) receptor system, Surf. Sci. 491 (2001) 433–443.
[39] M. Carrion-Vazquez, A.F. Oberhauser, S.B. Fowler, P.E. Marszalek, S.E. Broedel, J. Clarke, J.M. Fernandez, Mechanical and chemical unfolding of a single protein: a comparison, Proc. Natl. Acad. Sci. U.S.A. 96 (1999) 3694–3699.
[40] M. Rief, M. Gautel, F. Oesterhelt, J.M. Fernandez, H.E. Gaub, Reversible unfolding of individual titin immunoglobulin domains by AFM, Science 276 (1997) 1109–1112.
[41] C. Bustamante, J.F. Marko, E.D. Siggia, S. Smith, Entropic elasticity of lambda-phage DNA, Science 265 (1994) 1599–1600.
[42] A. Sethuraman, M. Han, R.S. Kane, G. Belfort, Effect of surface wettability on the adhesion of proteins, Langmuir 20 (2004) 7779–7788.
[43] P.L. Privalov, L.V. Medved', Domains in the fibrinogen molecule, J. Mol. Biol. 159 (1982) 665–683.
[44] L.C. Xu, C.A. Siedlecki, Effects of surface wettability and contact time on protein adhesion to biomaterial surfaces, Biomaterials 28 (2007) 3273–3283.
[45] R.E. Marchant, A.S. Lea, J.D. Andrade, P. Bockenstedt, Interactions of Vonwillebrand-factor on mica studies by atomic force microscopy, J. Colloid Interf. Sci. 148 (1992) 261–272.
[46] C.A. Siedlecki, S.J. Eppell, R.E. Marchant, Interactions of human Von-Willebrand-factor with a hydrophobic self-assembled monolayer studied by atomic-force microscopy, J. Biomed. Mater. Res. 28 (1994) 971–980.
[47] G.I. Bell, Models for the specific adhesion of cells to cells, Science 200 (1978) 618–627.
[48] S. Tsuboi, Calcium integrin-binding protein activates platelet integrin alpha IIbbeta 3, J. Biol. Chem. 277 (2002) 1919–1923, doi:10.1074/jbc.M110643200.